Fifteenth USA/Europe Air Traffic Management Research and Development Seminar (ATM2023)

# Towards Multi-Aircraft Transfer Learning for Trajectory Tracking

Almudena Buelta, Alberto Olivares, and Ernesto Staffetti
Department of Signal Theory and Communications and Telematic Systems and Computing
Universidad Rey Juan Carlos
Fuenlabrada, Madrid, Spain
almudenajose.buelta@urjc.es, alberto.olivares@urjc.es, ernesto.staffetti@urjc.es

***Abstract*—In this paper, a control method that combines model reference adaptive control (MRAC) and iterative learning control (ILC) is applied to aircraft trajectory tracking. ILC is intended for repetition-invariant system dynamics, in which the nominal dynamic model of the aircraft is assumed to be known. However, in real operations, this requirement is not met, as different aircraft perform consecutive flights along the same trajectory. To address this limitation, a multi-aircraft transfer learning strategy is proposed, which allows the learned trajectory knowledge to be transferred to dynamically different aircraft at each iteration. In order to achieve this, the aircraft's baseline controller is augmented with an MRAC, which drives the system's performance close to that of a reference model, and an ILC, which serves as a high-level adaptation scheme to compensate for repetitive disturbances. According to the preliminary results obtained from experiments carried out with various simulated aircraft, taking into account model uncertainties, disturbances, and changing dynamics, the performance of the ILC in combination with the MRAC augmentation of a baseline controller is superior to that of the baseline controller without MRAC augmentation. After a few iterations, a significant reduction in the trajectory tracking error is observed, with only small fluctuations occurring throughout the subsequent iterations. As a result, the MRAC- ILC combination makes the ILC applicable to real operations, improves the predictability of aircraft trajectories, and enhances the efficiency of the air traffic management system.**

***Keywords*—Aircraft trajectory tracking, iterative learning control, model reference adaptive control, transfer learning, trajectory predictability.**

## I. Introduction

Air Traffic Management (ATM) is experiencing a transformation to adapt the air navigation system to the increasing air traffic demand. This new ATM paradigm is built on trajectory-based operations (TBO), in which the trajectories are optimized based on the preferences of the airlines. Trajectory predictability, namely the correspondence between the planned and flown trajectories, is key to implementing TBOs, which require high precision in aircraft trajectory tracking. Higher trajectory predictability implies better traffic synchronization, which results in an improvement in the safety, efficiency, and capacity of the ATM system. However, due to multiple random factors, such as wind and temperature forecast errors or unpredictable weather events (mainly storms), some level of uncertainty remains, hindering precision and resulting in deviations from the planned trajectory that can neither be predicted nor compensated by usual aircraft trajectory tracking controllers.

This article presents the preliminary results of a multi-aircraft transfer learning method in which Model Reference Adaptive Control (MRAC) and Iterative Learning Control (ILC) are combined to achieve precise aircraft trajectory tracking. In [1], an optimization-based ILC scheme is applied to trajectory tracking for commercial aircraft, demonstrating the effectiveness of this approach to compensate for disturbances in the presence of operational constraints when consecutive flights are carried out by identical aircraft. However, in a realistic scenario, additional difficulties arise because consecutive flights are generally performed by different aircraft. For instance, in airport departure and arrival procedures, it is typical for different aircraft to follow very similar routes. Furthermore, the dynamic models of these aircraft may not be fully known since the estimation of certain parameters, such as the aircraft's initial mass, may not be accurate. Therefore, a realistic assumption is that different dynamical systems perform each iteration, whereas the basic ILC scheme requires the system dynamics to be repetition-invariant. This drawback is overcome in this article by using an underlying adaptive controller that forces the aircraft to behave close to a specified reference model. In the experiments described in this article, the chosen reference model is the same aircraft model as the one for which the trajectory to be followed is designed, which is an A320. In particular, an MRAC is combined with the aircraft's preexisting trajectory tracking controller, in this case, a Linear Quadratic Regulator (LQR) Proportional Integral (PI) controller, enhancing its performance through direct adaptation. The introduction of the MRAC in ILC allows learned trajectory knowledge to be transferred among different systems. In the context of this article, the knowledge to be transferred includes the reference trajectory and the estimated disturbances.

### A. Previous approaches

The transfer learning method proposed here, combining adaptive control and learning control, has been explored in other works. In [2], a model reference adaptive ILC strategy is

This work has been partially supported by the grants number RTI2018-098471-B-C33 and PID2021-122323OB-C31 of the Spanish Government.

presented for single-input single-output linear time-invariant robot manipulators with unknown parameters, performing repetitive tasks, through a discrete-type parametric adaptation law that refines the transient response from iteration to iteration. ILC is combined with an MRAC strategy in [3] to design a control parameter adaptive law, in which the parameters of the control systems at each iteration are adapted based on the results of previous iterations. In [4], a reinforcement learning-based flight control system is designed to improve the transient response performance of a closed-loop model reference adaptive control system. A combination of $\mathcal{L}_1$ adaptive feedback control with parallel ILC is proposed in [5], where the combination of $\mathcal{L}_1$ and ILC is successfully applied to a simulated system. In this work, ILC ensures that the plant uncertainty is sufficiently small for the $\mathcal{L}_1$ controller, which is in charge of precision motion control, to compensate for parametric uncertainties. In [6], experimental results are reported for a serial combination of $\mathcal{L}_1$ adaptive control and ILC for quadrotor trajectory tracking under changing dynamics. The knowledge acquired by the ILC algorithm over iterations is transferred across different systems, since the $\mathcal{L}_1$ adaptive controller copes with the underlying changes in the system dynamics.

In this paper, a serial MRAC-ILC architecture is proposed, in which an MRAC augmentation of a baseline controller is used as an underlying controller to achieve robust, repeatable behavior, whereas the ILC acts as a high-level adaptation scheme and compensates for repetitive disturbances. This approach is based on the $\mathcal{L}_1$-ILC method presented in [7], in which it is proven that this technique enables transfer learning between dynamically different systems, where the experience gained by one system serves another system to achieve high accuracy in trajectory tracking.

The experiments presented in this paper show the behavior of the MRAC-ILC scheme when the aircraft are affected by model uncertainties and changing dynamics between iterations, but also disturbances that cause them to deviate from the planned trajectory. The ILC compensates for the repetitive disturbances that are too severe for the MRAC to correct. In these experiments, these strong disturbances represent the wind, assuming it remains constant throughout the iterations. A more general approach to addressing this problem within the ILC can be found in [8], where recursive Gaussian process regression is introduced in the ILC algortihm to estimate and predict repetitive disturbances even if they vary between iterations, including the horizontal wind.

### B. Contributions of the paper

In this paper, an MRAC augmentation of a feedback baseline controller robust to disturbances is combined with ILC, showing its ability to improve trajectory tracking by learning from previous iterations and, at the same time, transfer the knowledge acquired in the previous iterations among dynamically different aircraft, since the MRAC forces them to behave in a similar way, whereas the ILC improves the tracking performance even in the presence of repetitive disturbances.

Therefore, the transfer learning method proposed in this paper is able to improve the tracking performance of commercial aircraft in following their planned trajectories. Trajectory predictability is thus enhanced, facilitating the implementation of TBOs in busy airports and reducing the number of alterations when following the planned trajectories, which entails an increase in the efficiency of the ATM system, resulting in a reduction of costs and emissions.

### C. Organization of the paper

A general overview of the optimization-based ILC method is given in Section II. In Section III the design of the MRAC augmentation of an LQR PI controller for a commercial aircraft is described. Section IV presents the learning-based controller, in which the ILC is used in combination with the MRAC. The results of the numerical experiments reported in Section V show that the MRAC-ILC combination is able to transfer the learned trajectory knowledge to dynamically different aircraft, achieving high-accuracy trajectory tracking. Finally, in Section VI some conclusions are drawn, and possible future lines of research are outlined.

## II. Iterative Learning Control

In this section, following [1], the optimization-based ILC scheme presented in [9] is summarized.

The ILC problem is solved in two steps, both relying on a nominal model of the aircraft, in which input and state constraints are explicitly taken into account. The first step consists in the estimation of the model errors and external disturbances affecting the flight of an aircraft along a trajectory using a time-varying Kalman filter. In the second step, optimization techniques are employed to determine an updated control input for the following aircraft, which optimally compensates for the recurrent disturbances in tracking the same trajectory.

It is assumed that an approximate model of the system is known in the form

$$\begin{aligned} \dot{\mathbf{x}}(t) &= \mathbf{f}(\mathbf{x}(t), \mathbf{u}(t), t), \\ \mathbf{y}(t) &= \mathbf{h}(\mathbf{x}(t), \mathbf{u}(t), t), \end{aligned} \tag{1}$$

where $\mathbf{x}(t) \in \mathbb{R}^{n_x}$ and $\dot{\mathbf{x}}(t) \in \mathbb{R}^{n_x}$ are the state and the state's derivative, respectively, $\mathbf{u}(t) \in \mathbb{R}^{n_u}$ is the control input, $\mathbf{y}(t) \in \mathbb{R}^{n_y}$ is the output, and $\mathbf{f}(\cdot)$ and $\mathbf{h}(\cdot)$ are assumed to be continuously differentiable in $\mathbf{x}$ and $\mathbf{u}$.

The output, state, and input signals are discretized and the deviations with respect to the desired output trajectory and its corresponding state and input, $\tilde{\boldsymbol{y}}(t) = \mathbf{y}(t) - \mathbf{y_d}(t)$, $\tilde{\boldsymbol{x}}(t) = \mathbf{x}(t) - \mathbf{x_d}(t)$, and $\tilde{\boldsymbol{u}}(t) = \mathbf{u}(t) - \mathbf{u_d}(t)$, are then lifted as stacked vectors of all discretization time-steps ( [10], [11]), obtaining the triple of lifted vectors $(\boldsymbol{x}, \boldsymbol{u}, \boldsymbol{y})$.

$$\begin{aligned} \boldsymbol{x}_j &= \boldsymbol{F}\boldsymbol{u}_j + \boldsymbol{d}_j, \\ \boldsymbol{y}_j &= \boldsymbol{G}\boldsymbol{x}_j + \boldsymbol{H}\boldsymbol{u}_j, \end{aligned} \tag{2}$$

where the subscript $j$ indicates the $j-$th execution of the desired task, $\boldsymbol{d}_j$ captures the repetitive disturbances along the reference trajectory, including model errors and the free response of the system to the initial deviation, and the

constant matrices $\boldsymbol{F}$, $\boldsymbol{G}$, and $\boldsymbol{D}$ are derived from the nominal model.

The disturbances $\boldsymbol{d}_j$ are initially unknown and need to be estimated based on measurements from previous iterations to compute the predicted disturbances for the following iteration, $\boldsymbol{d}^p_{j+1}$. As in [9], an iteration-domain Kalman filter is used here to compute the estimate of the vector $\boldsymbol{d}_j$, which is assumed to experience only slight random changes between iterations.

The updated input that minimizes the deviation from the desired trajectory in the following iteration, $\boldsymbol{u}_{j+1}$, is computed solving an optimization problem. The update rule can be expressed as

$$\begin{aligned} \min_{\boldsymbol{u}_{j+1}} \quad & \|\boldsymbol{F}\boldsymbol{u}_{j+1} + \boldsymbol{d}^p_{j+1}\|_\ell + \alpha\|\boldsymbol{D}\boldsymbol{u}_{j+1}\|_\ell, \\ \text{subject to:} \quad & \boldsymbol{L}\boldsymbol{u}_{j+1} \leq \boldsymbol{q}_{\max}, \end{aligned}$$

where vector $\boldsymbol{q}_{\max}$ and matrix $\boldsymbol{L}$ have appropriate dimensions and capture the system constraints. $\alpha \geq 0$ and $\boldsymbol{D}$ are introduced to penalize the input or approximations of its derivatives in order to enforce the smoothness of the optimal problem solution.

As explained in the introduction, an indirect ILC approach is used since a new reference trajectory is computed and fed into the system's underlying trajectory tracking controller rather than a control input. In the experiments in Section V, the underlying controller is an MRAC augmentation of an LQR PI controller, which converts the reference trajectory into the system control inputs. The new reference trajectory is obtained as

$$\begin{aligned} \boldsymbol{x}_r &= \boldsymbol{F}\boldsymbol{u}_{j+1} + \boldsymbol{x}_d, \\ \boldsymbol{y}_r &= \boldsymbol{G}\boldsymbol{x}_r + \boldsymbol{H}\boldsymbol{u}_{j+1} + \boldsymbol{y}_d, \end{aligned}$$

where $\boldsymbol{x}_r \in \mathbb{R}^{Nn_x}$ and $\boldsymbol{y}_r \in \mathbb{R}^{Nn_y}$ are, respectively, the new reference state and output lifted vectors, and $\boldsymbol{x}_d \in \mathbb{R}^{Nn_x}$ and $\boldsymbol{y}_d \in \mathbb{R}^{Nn_y}$ are, respectively, the desired state and output vectors also in a lifted form. The reference trajectory, $\mathbf{r}_{j+1}$ to be fed to the MRAC augmentation of the baseline LQR PI controller in the following iteration can be obtained from the unlifted representation form of $\boldsymbol{x}_r$ and $\boldsymbol{y}_r$.

## III. MRAC AUGMENTATION OF A BASELINE CONTROLLER

In the experiments in Section V, an LQR PI + MRAC controller is designed to be implemented into the flight simulator of a commercial aircraft. The LQR baseline controller with PI action stabilizes the aircraft dynamics and regulates the speed and altitude of the aircraft under nominal conditions, and the MRAC acts as an augmentation control signal to mitigate the system uncertainties. The extended architecture used in this paper is identical to the one proposed in [12, Chap. 11.5]. This augmentation approach enables the use of adaptive control, improving the performance of the aircraft's baseline feedback controller, in this case, the LQR PI baseline controller, instead of replacing it.

A MIMO nonlinear uncertain system is considered in the form

$$\begin{aligned} \dot{\boldsymbol{x}}_{\boldsymbol{p}} &= \boldsymbol{A}_{\boldsymbol{p}}\boldsymbol{x}_{\boldsymbol{p}} + \boldsymbol{B}_{\boldsymbol{p}}\boldsymbol{\Lambda}\left(\boldsymbol{u} + \boldsymbol{f}(\boldsymbol{x}_{\boldsymbol{p}})\right), \\ \boldsymbol{y} &= \boldsymbol{C}_{\boldsymbol{p}}\boldsymbol{x}_{\boldsymbol{p}}, \end{aligned} \tag{3}$$

with

$$\boldsymbol{f}(\boldsymbol{x}_{\boldsymbol{p}}) = \boldsymbol{\Theta}^T\boldsymbol{\Phi}(\boldsymbol{x}_{\boldsymbol{p}}), \tag{4}$$

where $\boldsymbol{x}_{\boldsymbol{p}} \in \mathbb{R}^{n_p}$ is the system state vector, $\boldsymbol{u} \in \mathbb{R}^m$ is the control input, and $\boldsymbol{y}_{\boldsymbol{p}} \in \mathbb{R}^m$ is the system regulated output. $\boldsymbol{B}_{\boldsymbol{p}} \in \mathbb{R}^{n_p \times m}$ and $\boldsymbol{C}_{\boldsymbol{p}} \in \mathbb{R}^{m \times n_p}$ are known and constant matrices, $\boldsymbol{A}_{\boldsymbol{p}} \in \mathbb{R}^{n_p \times n_p}$ is an unknown and constant matrix, and $\boldsymbol{\Lambda} \in \mathbb{R}^{m \times m}$ is a constant diagonal unknown matrix with positive diagonal elements. The pair $(\boldsymbol{A}_{\boldsymbol{p}}, \boldsymbol{B}_{\boldsymbol{p}}\boldsymbol{\Lambda})$ is assumed to be controllable. $\boldsymbol{f}(\boldsymbol{x}) \in \mathbb{R}^m$ is the matched uncertainty, where $\boldsymbol{\Theta} \in \mathbb{R}^{N \times m}$ is the matrix of unknown and constant parameters, and $\boldsymbol{\Phi}(\boldsymbol{x}_{\boldsymbol{p}}) \in \mathbb{R}^N$ is a known regressor vector, whose components are locally Lipschitz-continuous functions of $\boldsymbol{x}_{\boldsymbol{p}}$.

The control goal is to design a control input, $\boldsymbol{u}$, such that the system regulated output tracks any bounded time-varying command, $\boldsymbol{r}(t) \in \mathbb{R}^m$, with bounded errors and in the presence of the system uncertainties $\{\boldsymbol{A}_{\boldsymbol{p}}, \boldsymbol{\Lambda}, \boldsymbol{\Theta}\}$.

Introducing the system output tracking error, $\boldsymbol{e}_{\boldsymbol{y}} = \boldsymbol{y}(t) - \boldsymbol{r}(t)$, into (3) yields to the extended open-loop dynamics

$$\begin{aligned} \dot{\boldsymbol{x}} &= \boldsymbol{A}\boldsymbol{x} + \boldsymbol{B}\boldsymbol{\Lambda}\left(\boldsymbol{u} + \boldsymbol{\Theta}^T\boldsymbol{\Phi}(\boldsymbol{x}_{\boldsymbol{p}})\right) + \boldsymbol{B}_{\boldsymbol{m}}\boldsymbol{r}, \\ \boldsymbol{y} &= \boldsymbol{C}\boldsymbol{x}, \end{aligned} \tag{5}$$

in which the integrated output tracking error

$$\boldsymbol{e}_{\boldsymbol{yI}}(t) = \int_0^t \boldsymbol{e}_{\boldsymbol{y}}(\tau)d\tau \tag{6}$$

is appended to the state vector, whose dimension becomes $n = n_p + m$. The extended state vector is $\boldsymbol{x} = \begin{pmatrix} \boldsymbol{e}^T_{\boldsymbol{yI}} & \boldsymbol{x}^T_{\boldsymbol{p}} \end{pmatrix}^T \in \mathbb{R}^n$. The extended open-loop system matrices in (5) are then

$$\begin{aligned} \boldsymbol{A} &= \begin{pmatrix} \boldsymbol{0}_{m\times m} & \boldsymbol{C}_{\boldsymbol{p}} \\ \boldsymbol{0}_{n_p\times m} & \boldsymbol{A}_{\boldsymbol{p}} \end{pmatrix}, \quad \boldsymbol{B} = \begin{pmatrix} \boldsymbol{0}_{m\times m} \\ \boldsymbol{B}_{\boldsymbol{p}} \end{pmatrix}, \\ \boldsymbol{B}_{\boldsymbol{m}} &= \begin{pmatrix} -\boldsymbol{I}_{m\times m} \\ \boldsymbol{0}_{n_p\times m} \end{pmatrix}, \qquad \boldsymbol{C} = \begin{pmatrix} \boldsymbol{0}_{m\times m} & \boldsymbol{C}_{\boldsymbol{p}} \end{pmatrix}. \end{aligned} \tag{7}$$

Since nominal operating conditions are assumed for the extended system, namely $\boldsymbol{\Lambda} = \boldsymbol{I}_{m\times m}$ and $\boldsymbol{\Theta} = \boldsymbol{0}_{N\times m}$, the control law is

$$\boldsymbol{u}_{bl} = -\boldsymbol{K}^T_{\boldsymbol{x}}\boldsymbol{x} = -\boldsymbol{K}_{\boldsymbol{I}}\boldsymbol{e}_{\boldsymbol{yI}} - \boldsymbol{K}_{\boldsymbol{P}}\boldsymbol{x}_{\boldsymbol{p}}, \tag{8}$$

in which the gain matrix $\boldsymbol{K}_{\boldsymbol{x}}$ is partitioned into the integral gain $\boldsymbol{K}_{\boldsymbol{I}}$ and the proportional gain $\boldsymbol{K}_{\boldsymbol{P}}$ and designed using an optimal control technique, namely an LQR.

The tracking performance of the LQR PI controller may deteriorate in the presence of the system uncertainties. An augmented adaptive controller is designed in order to restore the expected behavior. The design entails defining the reference model, formulating the tracking dynamics, and determining the adaptive laws. The design of the augmented adaptive controller is explained in [12, Sec. 10.3]. The main steps are reported here for convenience.

Given a reference Hurwitz matrix $\boldsymbol{A}_{\boldsymbol{m}}$ and an unknown positive-definite diagonal constant matrix $\boldsymbol{\Lambda}$, it is assumed that there exists a constant and possibly unknown gain matrix $\boldsymbol{K}_{\boldsymbol{x}} \in \mathbb{R}^{n\times m}$, such that

$$\boldsymbol{A}_{\boldsymbol{m}} = \boldsymbol{A} + \boldsymbol{B}\boldsymbol{\Lambda}\boldsymbol{K}^T_{\boldsymbol{x}}. \tag{9}$$

The reference model representative of the baseline closed-loop system dynamics is

$$\begin{aligned} \dot{\boldsymbol{x}}_{\boldsymbol{m}} &= \boldsymbol{A}_{\boldsymbol{m}}\boldsymbol{x}_{\boldsymbol{m}} + \boldsymbol{B}_{\boldsymbol{m}}\boldsymbol{r}, \\ \boldsymbol{y}_{\boldsymbol{m}} &= \boldsymbol{C}\boldsymbol{x}_{\boldsymbol{m}}, \end{aligned} \tag{10}$$

so that the extended system dynamics in (5) can be expressed as

$$\dot{\boldsymbol{x}} = \boldsymbol{A}_{\boldsymbol{m}}\boldsymbol{x} + \boldsymbol{B}\boldsymbol{\Lambda}\left(\boldsymbol{u} - \boldsymbol{K}_{\boldsymbol{x}}^T\boldsymbol{x} + \boldsymbol{\Theta}^T\boldsymbol{\Phi}(\boldsymbol{x}_{\boldsymbol{p}})\right) + \boldsymbol{B}_{\boldsymbol{m}}\boldsymbol{r}. \tag{11}$$

The control input is then the sum of the baseline component, $\boldsymbol{u}_{bl}$, and its adaptive augmentation, $\boldsymbol{u}_{ad}$,

$$\boldsymbol{u} = -\boldsymbol{K}_{\boldsymbol{x}}^T\boldsymbol{x} + \boldsymbol{u}_{ad} = \boldsymbol{u}_{bl} + \boldsymbol{u}_{ad}. \tag{12}$$

Substituting (12) into the system dynamics (11) yields

$$\dot{\boldsymbol{x}} = \boldsymbol{A}_{\boldsymbol{m}}\boldsymbol{x} + \boldsymbol{B}\boldsymbol{\Lambda}\left(\boldsymbol{u}_{ad} + \bar{\boldsymbol{\Theta}}^T\bar{\boldsymbol{\Phi}}(\boldsymbol{u}_{bl}, \boldsymbol{x}_{\boldsymbol{p}})\right) + \boldsymbol{B}_{\boldsymbol{m}}\boldsymbol{r}, \tag{13}$$

where the regressor vector and the matrix of unknown parameters are redefined as

$$\bar{\boldsymbol{\Phi}}(\boldsymbol{u}_{bl}, \boldsymbol{x}_{\boldsymbol{p}}) = \begin{pmatrix} \boldsymbol{u}_{bl}^T & \boldsymbol{\Phi}^T(\boldsymbol{x}_{\boldsymbol{p}}) \end{pmatrix}^T, \quad \bar{\boldsymbol{\Theta}} = \begin{pmatrix} \boldsymbol{K}_{\boldsymbol{u}}^T & \boldsymbol{\Theta}^T \end{pmatrix}^T, \tag{14}$$

with $\boldsymbol{K}_{\boldsymbol{u}}^T = \boldsymbol{I}_{m\times m} - \boldsymbol{\Lambda}^{-1}$. The adaptive control component is designed to compensate for the system uncertainty

$$\boldsymbol{u}_{ad} = -\hat{\bar{\boldsymbol{\Theta}}}^T\bar{\boldsymbol{\Phi}}(\boldsymbol{u}_{bl}, \boldsymbol{x}_{\boldsymbol{p}}), \tag{15}$$

where $\hat{\bar{\boldsymbol{\Theta}}} \in \mathbb{R}^{(N+n)\times m}$ is the matrix of adaptive parameters. Substituting (15) into (13) yields

$$\dot{\boldsymbol{x}} = \boldsymbol{A}_{\boldsymbol{m}}\boldsymbol{x} - \boldsymbol{B}\boldsymbol{\Lambda}\tilde{\bar{\boldsymbol{\Theta}}}^T\bar{\boldsymbol{\Phi}}(\boldsymbol{u}_{bl}, \boldsymbol{x}_{\boldsymbol{p}}) + \boldsymbol{B}_{\boldsymbol{m}}\boldsymbol{r}, \tag{16}$$

with $\tilde{\bar{\boldsymbol{\Theta}}} = \hat{\bar{\boldsymbol{\Theta}}} - \bar{\boldsymbol{\Theta}}$.

Given the state tracking error $\boldsymbol{e} = \boldsymbol{x} - \boldsymbol{x}_{\boldsymbol{m}}$, the tracking error dynamics are

$$\dot{\boldsymbol{e}} = \boldsymbol{A}_{\boldsymbol{m}}\boldsymbol{e} - \boldsymbol{B}\boldsymbol{\Lambda}\tilde{\bar{\boldsymbol{\Theta}}}^T\bar{\boldsymbol{\Phi}}. \tag{17}$$

Considering the positive-definite adaptation rate matrix $\boldsymbol{\Gamma}_{\bar{\boldsymbol{\Theta}}} = \boldsymbol{\Gamma}_{\bar{\boldsymbol{\Theta}}}^T > \boldsymbol{0}$, the adaptive law is obtained through the Lyapunov function candidate

$$V = \boldsymbol{e}^T\boldsymbol{P}\boldsymbol{e} + \operatorname{Tr}\left(\tilde{\bar{\boldsymbol{\Theta}}}^T\boldsymbol{\Gamma}_{\bar{\boldsymbol{\Theta}}}^{-1}\tilde{\bar{\boldsymbol{\Theta}}}\boldsymbol{\Lambda}\right), \tag{18}$$

where $\boldsymbol{P} = \boldsymbol{P}^T > \boldsymbol{0}$ is the solution of the algebraic Lyapunov equation

$$\boldsymbol{P}\boldsymbol{A}_{\boldsymbol{m}} + \boldsymbol{A}_{\boldsymbol{m}}^T\boldsymbol{P} = -\boldsymbol{Q}, \tag{19}$$

for some $\boldsymbol{Q} = \boldsymbol{Q}^T > \boldsymbol{0}$. The time derivative of $V$ is then

$$\dot{V} = -\boldsymbol{e}^T\boldsymbol{Q}\boldsymbol{e} + 2\operatorname{Tr}\left(\tilde{\bar{\boldsymbol{\Theta}}}^T\left[\boldsymbol{\Gamma}_{\bar{\boldsymbol{\Theta}}}^{-1}\dot{\hat{\bar{\boldsymbol{\Theta}}}} - \bar{\boldsymbol{\Phi}}\boldsymbol{e}^T\boldsymbol{P}\boldsymbol{B}\right]\boldsymbol{\Lambda}\right). \tag{20}$$

To prove the uniform ultimate boundedness of $(\boldsymbol{e}, \tilde{\bar{\boldsymbol{\Theta}}})$, the adaptive laws are selected as

$$\dot{\hat{\bar{\boldsymbol{\Theta}}}} = \boldsymbol{\Gamma}_{\bar{\boldsymbol{\Theta}}}\bar{\boldsymbol{\Phi}}(\boldsymbol{u}_{\boldsymbol{bl}}, \boldsymbol{x}_{\boldsymbol{p}})\boldsymbol{e}^T\boldsymbol{P}\boldsymbol{B}, \tag{21}$$

leading to

$$\dot{V}(\boldsymbol{e}, \tilde{\bar{\boldsymbol{\Theta}}}) = -\boldsymbol{e}^T\boldsymbol{Q}\boldsymbol{e} \leq 0. \tag{22}$$

The adaptive laws in (21) can be written in terms of the original parameters as

$$\begin{aligned} \dot{\hat{\boldsymbol{K}}}_{\boldsymbol{u}} &= \boldsymbol{\Gamma}_{\boldsymbol{u}}\boldsymbol{u}_{bl}\boldsymbol{e}^T\boldsymbol{P}\boldsymbol{B}, \\ \dot{\hat{\boldsymbol{\Theta}}} &= \boldsymbol{\Gamma}_{\boldsymbol{\Theta}}\boldsymbol{\Phi}(\boldsymbol{x}_{\boldsymbol{p}})\boldsymbol{e}^T\boldsymbol{P}\boldsymbol{B}, \end{aligned} \tag{23}$$

where $\boldsymbol{\Gamma}_{\boldsymbol{u}}$ and $\boldsymbol{\Gamma}_{\boldsymbol{\Theta}}$ are the rates of adaptation for the uncertainties corresponding to $\boldsymbol{x}$ and $\boldsymbol{\Phi}(\boldsymbol{x}_{\boldsymbol{p}})$, with $\boldsymbol{\Gamma}_{\bar{\boldsymbol{\Theta}}} = \begin{pmatrix} \boldsymbol{\Gamma}_{\boldsymbol{u}} & \boldsymbol{0}_{n\times m} \\ \boldsymbol{0}_{N\times m} & \boldsymbol{\Gamma}_{\boldsymbol{\Theta}} \end{pmatrix}$. The total control input can also be expressed as

$$\boldsymbol{u} = \boldsymbol{u}_{bl} + \boldsymbol{u}_{ad} = -\boldsymbol{K}_{\boldsymbol{x}}^T\boldsymbol{x} + \left[-\hat{\boldsymbol{K}}_{\boldsymbol{u}}^T\boldsymbol{u}_{bl} - \hat{\boldsymbol{\Theta}}\boldsymbol{\Phi}^T(\boldsymbol{x}_{\boldsymbol{p}})\right]. \tag{24}$$

## IV. Combined MRAC-ILC method

As said earlier, the objective of the MRAC-ILC method is to force the controlled system to behave in a repeatable and reliable way, while achieving precise trajectory tracking despite the presence of model uncertainties, disturbances and changing dynamics. The MRAC makes the system performance repeatable, forcing it to behave close to a reference model, even if it is affected by model uncertainties and changing dynamics. However, the MRAC by itself may not suffice to drive the system along a desired trajectory if the model errors and disturbances affecting the system move it away from this trajectory. These disturbances represent the environmental conditions, such as wind. In this case, the ILC gradually compensates for repetitive disturbances improving the tracking performance of the controlled system over multiple executions of the task.

The transfer learning scheme is shown in Figure 1. Given two different closed-loop control systems, both equipped with an MRAC augmentation of a baseline controller with the same reference model, the objective of the second control system is to precisely track a desired trajectory, $\mathbf{y_d}$, based on the experience gained by the first control system. At iteration $j$, a previously computed commanded reference signal, $\mathbf{r}_j$, is fed to the adaptive controller of system 1, which generates a control action that, due to unmodelled dynamics and external disturbances, drives the system through an output signal $\mathbf{y}_{1,j}$ that may be deviated from the desired trajectory. The ILC estimates this deviation and optimally generates a new reference signal for the following iteration, $\mathbf{r}_{j+1}$. Since the adaptive controllers of the systems are designed using the same reference model, the signal $\mathbf{r}_{j+1}$ can be directly introduced into the controller of control system 2. The resulting output signal $\mathbf{y}_{2,j+1}$ incorporates the corrections determined by the ILC given the experience gathered by control system 1, achieving high performance on tracking the desired trajectory.

## V. Experimental results

In this section, the results of the application of the MRAC-ILC method to different trajectory tracking problems that involve different commercial aircraft are described.

The simulated performances of three different aircraft are considered in the numerical experiments, namely an Airbus A320-231 (A320), a Boeing 767-300ER (B767), and an Embraer ERJ 190-200 IGW (E195), which belong to

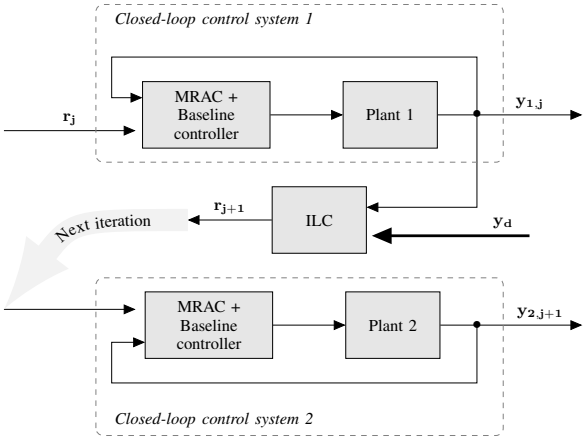


Figure 1: MRAC-ILC transfer learning block diagram. The closed-loop systems 1 and 2 are controlled by an MRAC augmentation of their baseline controllers with the same reference model. The ILC improves the trajectory tracking performance of system 2 by learning from the deviations suffered by system 1.

different classes, being a mid-sized aircraft, a large-to-mid-sized aircraft, and a mid-to-light-sized aircraft, respectively.

In this paper, a common 3-DOF dynamic model is considered, which describes the point variable-mass motion of the aircraft over a non-rotating flat earth model, in which the acceleration of gravity is constant and perpendicular to the surface of the earth, that is considered an approximate inertial reference frame. In particular, a symmetric flight is used. Thus, it is assumed that there is no sideslip and all the forces, namely propulsive, aerodynamic, and gravitational forces, lie in the plane of symmetry of the aircraft, which is a conventional jet airplane with fixed engines [13]. Only the vertical profile of the trajectories followed by the aircraft has been taken into account since the mission profiles for which airplanes are designed are primarily in the vertical plane. Therefore, the motion of the aircraft is limited to a vertical plane, namely with constant course and thus constant heading angle, which, without loss of generality, is assumed to be zero. In particular, a leveled-wing flight is considered, thus the bank angle is also zero. Additionally, it is assumed that there are no actions out of the vertical plane, and the wind component perpendicular to the plane of motion is zero.

Therefore, the equations of motion of the aircraft are:

$$\begin{aligned}
\dot{V}(t) &= \frac{T(t) - D(h_e(t), V(t), C_L(t)) - m(t) \cdot g \cdot \sin\gamma(t)}{m(t)}, \\
\dot{\gamma}(t) &= \frac{L(h_e(t), V(t), C_L(t)) - m(t) \cdot g \cdot \cos\gamma(t)}{m(t) \cdot V(t)}, \\
\dot{x}_e(t) &= V(t) \cdot \cos\gamma(t) + W_x(x_e(t), h_e(t)), \\
\dot{h}_e(t) &= V(t) \cdot \sin\gamma(t), \\
\dot{m}(t) &= -T(t) \cdot \eta(V(t)),
\end{aligned} \tag{25}$$

where $V$ is the true airspeed, $\gamma$ is the flight path angle, $x_e$ is the horizontal position, $h_e$ is the altitude, $m$ is the aircraft mass, $T$ is the engine thrust, and $C_L$ is the lift coefficient. The lift, $L = C_L S\hat{q}$, and the drag, $D = C_D S\hat{q}$, are the components of the aerodynamic force. Parameter $S$ is the reference wing surface area, and $\hat{q} = \frac{1}{2}\rho V^2$ is the dynamic pressure. A parabolic drag polar $C_D = C_{D0} + KC_L^2$ and an International Standard Atmosphere (ISA) model are assumed. The lift coefficient $C_L$ is a known function of the angle of attack $\alpha$ and the Mach number. Parameter $\eta$ is the fuel efficiency coefficient. Further details on the aircraft equations of motions and flight envelope can be found in [1]. The performance parameters of each aircraft have been obtained from the Eurocontrol's Base of Aircraft Data (BADA) [14].

The aim of the aircraft's underlying controller, namely the MRAC augmentation of the baseline LQR PI controller, is that two components of the output variables track those of a command signal $\mathbf{r}(t) = (V_{cmd}(t), h_{e,cmd}(t))$. Therefore, the output variables considered by the underlying controller are $\mathbf{y_{uc}}(t) = (V(t), h_e(t))$. The extended state vector of the underlying aircraft controller is $\mathbf{x_{uc}}(t) = (V_I(t), h_{eI}(t), V(t), \gamma(t), h_e(t))$, where $V_I(t)$ and $h_{eI}(t)$ are the integrated output tracking errors of the speed and the altitude, respectively, defined as in (6). The engine thrust, $T$, and the lift coefficient, $C_L$, are the control variables for the LQR PI controller, thus the control vector is $\boldsymbol{u}(t) = (T(t), C_L(t))$. The thrust is commanded by the engine throttle, and the lift coefficient can be considered linearly related to the angle of attack, which is commanded by the elevator trims.

The reference signal is computed at each iteration by the ILC in such a way that all the components of the output of the plant follow a desired trajectory $\mathbf{y_d}(t) = (V_d(t), \gamma_d(t), x_{e,d}(t), h_{e,d}(t), m_d(t))$. At each iteration, the ILC estimates the deviations of the actual output trajectory of the plant from the desired output trajectory using a Kalman filter. The ILC takes into account all the state variables of the plant model (25), namely $\mathbf{x}(t) = (V(t), \gamma(t), x_e(t), h_e(t), m(t))$, which are assumed to be directly measurable, thus the output vector of the plant used by the ILC is $\mathbf{y}(t) = \mathbf{x}(t)$.

The following errors are used to evaluate the performance of both the underlying controller and the ILC:

- The state tracking error measures the performance of the MRAC augmentation of the LQR PI in following the reference model. The norm of the state tracking error at each time step is calculated as the norm of the difference between the states of the plant model and the reference model, namely as $\|\mathbf{x_{uc}} - \mathbf{x_m}\|_2$, being $\mathbf{x_m}$ the extended state of the reference aircraft model.
- The weighted state error characterizes the performance of the MRAC-ILC method in following the desired trajectory at each iteration, scaled by a weighting matrix $\boldsymbol{S}$, that is

  $$e_{ws,j} = \|\boldsymbol{S}\boldsymbol{y}_j\|_2,$$

  where $\boldsymbol{y}_j$ is the lifted output error vector of the ILC at iteration $j$. The weighted scaling matrix, $\boldsymbol{S}$, is used to assign larger weights to the output errors of the position variables of the aircraft to achieve better precision in these output variables.

### A. Numerical results

The following three trajectory tracking experiments are carried out.

*1) Experiment 1: MRAC augmentation of a baseline LQR PI controller with a mismatch between reference and plant models:* The goal of this experiment is to demonstrate the capability of the MRAC to force different aircraft to behave as a common reference model. The reference model in the MRAC controller is that of an A320 aircraft with a baseline LQR PI controller. The plant model is that of a B767 aircraft, which is assumed to be not affected by external disturbances. Since external disturbances do not affect the plant, only the first iteration of the ILC is executed. This amounts to not using the ILC controller and testing only the closed-loop control system 1 in Figure 1. The reference signal $\mathbf{r}_1$ is composed of a series of steps of different magnitude for both the speed and altitude of the B767 aircraft. This trajectory does not correspond to any phase of a real flight operation. It has been chosen to demonstrate the effectiveness of the method in a fictitious yet feasible operation as a preliminary result to be further investigated on more realistic trajectories.

In Figure 2, the black dashed lines represent the reference speed and altitude to be tracked, the dotted gray lines represent the outputs of the reference model, which is that of an A320 aircraft, and the blue lines represent the outputs of the plant model, which is that of a B767 aircraft, using the MRAC augmentation of the baseline LQR PI controller. Finally, the orange lines represent the outputs of the plant model when only the baseline LQR PI controller is employed. As expected, since the baseline controller is designed for an A320 aircraft, its tracking performance on the plant model, which is a B767 aircraft, shows significant deviations when the MRAC is not used. On the contrary, when the MRAC is used, its tracking performance on the plant model is similar to the performance of the baseline LQR PI controller on the reference model.

Figure 3 shows the norms of the state tracking errors observed at each time step using the MRAC augmentation of the baseline LQR PI controller and the LQR PI baseline controller without MRAC augmentation. The norm of the state tracking error confirms that the state tracking error is considerably higher when only the baseline controller is active, as compared to the state tracking error when using the MRAC augmentation of the baseline controller.

The results of this experiment serve as the basis for the following experiments, in which external disturbances affecting the plant are considered. Therefore, the whole MRAC-ILC method is applied, in which the ILC iteratively compensates for the external disturbances and the MRAC allows the iterations to be carried out by different aircraft.

*2) Experiment 2: MRAC-ILC with transfer learning between two aircraft:* The goal of this experiment is to test the effectiveness of the whole MRAC-ILC method in Figure 1 when two different aircraft perform each iteration of the tracking task, wherein the iterations correspond to the consecutive flights undertaken by the aircraft trying to follow the planned trajectory. The reference model in the MRAC is that of an A320 aircraft with a baseline LQR PI

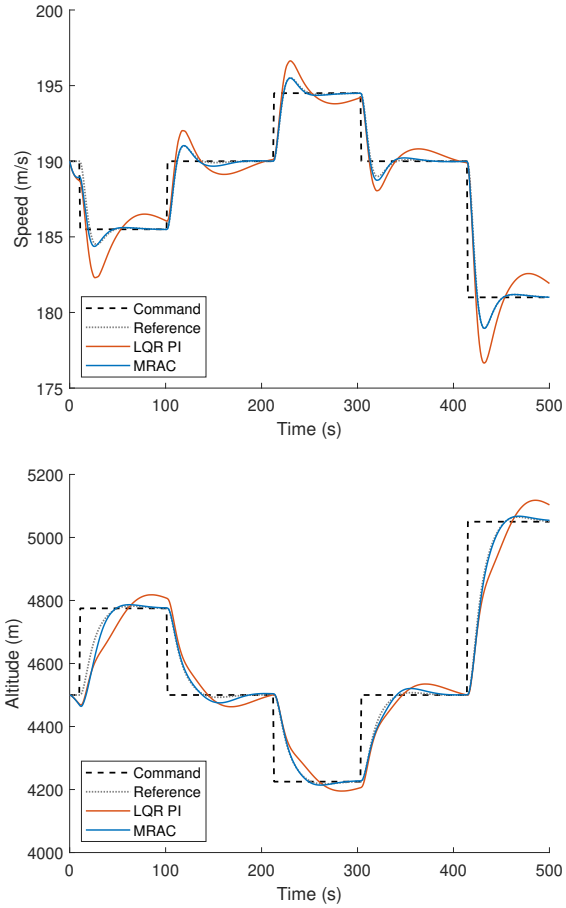


Figure 2: Experiment 1: Output tracking performances of the plant using the MRAC augmentation of a baseline LQR PI controller and the LQR PI controller without MRAC augmentation. The reference model of the MRAC is an A320 aircraft and the plant model is a B767 aircraft.

controller. In this experiment, the plant model is assumed to be affected by external disturbances. Specifically, horizontal wind and measurement errors are introduced. Since external disturbances affect the plant, several iterations of the ILC are executed. This amounts to using the whole MRAC-ILC method in Figure 1.

To make the scenario of this experiment more realistic, since successive flights on the same flight route are operated by different aircraft, the plant model is assumed to change during the iterations of the ILC. Specifically, the plant model is that of an A320 aircraft for the first nine iterations of the ILC. Afterwards, it changes to that of a B767 aircraft for the last eleven iterations of the ILC.

The ultimate goal of this experiment is to prove that the deviations from the desired output trajectory experienced by the plant due to repetitive disturbances can be amended by the ILC over iterations, learning from the deviations observed in previous executions of the tracking task, even if they are performed by two different aircraft.

In this experiment, the desired trajectory to be followed by the plant, $\mathbf{y_d}(t)$, is the feasible trajectory flown by the

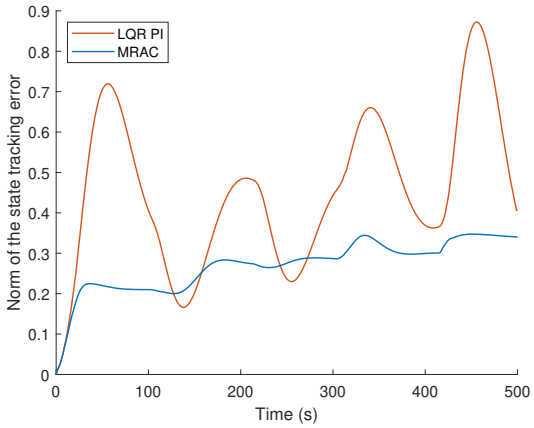


Figure 3: Experiment 1: Norms of the state tracking errors observed using the MRAC augmentation of a baseline LQR PI controller and the LQR PI baseline controller without MRAC augmentation. The reference model of the MRAC is an A320 aircraft and the plant model is a B767 aircraft.

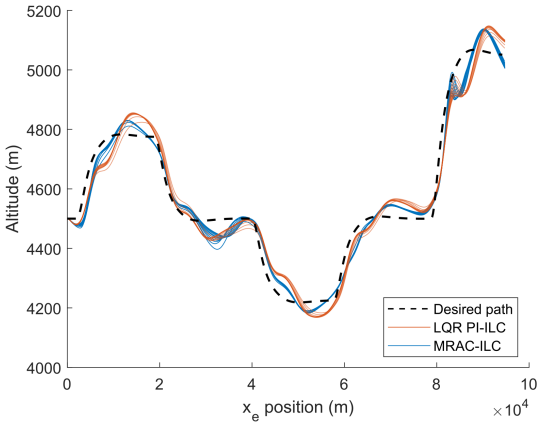


Figure 5: Experiment 2: Evolution of the path $x_e - h_e$ of the plant from iteration 10 on, after the plant model switch, using the ILC in combination with the MRAC augmentation of a baseline LQR PI controller and the LQR PI controller without MRAC augmentation.

reference aircraft, which is the A320 aircraft, in Experiment 1, in the absence of wind. The corresponding desired speed and altitude components are the command signals for the MRAC augmentation of the baseline LQR PI at the first iteration, namely $\mathbf{r}_1(t) = (V_d(t), h_{e,d}(t))$. In the subsequent iterations, the command signals are updated by the ILC.

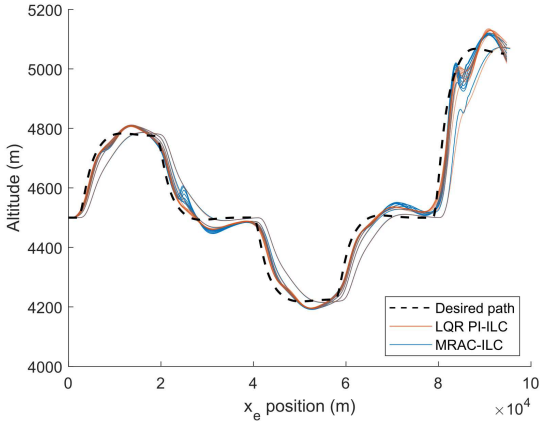


Figure 4: Experiment 2: Evolution of the path $x_e - h_e$ of the plant from iteration 1 to 9, before the plant model switch, using the ILC in combination with the MRAC augmentation of a baseline LQR PI controller and the LQR PI controller without MRAC augmentation.

Figures 4 and 5 show the evolution of the path $x_e - h_e$ over iterations using the ILC in combination with the MRAC augmentation of a baseline LQR PI controller and the LQR PI controller without MRAC augmentation. In Figure 4, only the results of the first nine iterations are reported, for which both control schemes show similar behavior since there is a concordance between the reference and the plant models. Figure 5 shows the results obtained using both schemes from iteration 10 on, when the plant model switches to that of a B767. It can be seen that the path followed by the aircraft differs depending on the control strategy, remaining closer to the desired path when the baseline controller is augmented with the MRAC.

Figures 6 and 7 show the evolution of the altitude and the speed of the plant over the first nine iterations and the remaining eleven iterations, respectively, using the ILC in combination with the MRAC augmentation of a baseline LQR PI controller and the LQR PI controller without MRAC augmentation. As shown in Figure 6, the plant exhibits a similar behavior in the first iterations when the plant and the reference models coincide. At the first iteration, the tracking of the speed is quite accurate, but due to the greater importance given to precision in position than precision in speed in the ILC algorithm, the precision in tracking the desired speed is sacrificed in favor of the precision in tracking both the horizontal position and the altitude. It can be observed in Figure 6 that only the latter tends to the desired altitude over the iterations, whereas the speed remains below the desired value. It can be observed in Figure 7 that from iteration 10, the behavior in speed and altitude tracking differ depending on the control strategy. The flown altitude is closer to the desired one when using the MRAC augmentation of a baseline LQR PI controller than without MRAC augmentation, and the speed is similar in both cases since precision in the position variables takes precedence over precision in the rest of the variables.

Figure 8 shows the evolution of the weighted state error over iterations using the ILC in combination with the MRAC augmentation of the baseline LQR PI controller and the LQR PI baseline controller without MRAC augmentation. As explained before, the weighted state error represents the difference between the desired and actual trajectories, where each component of the error vector is multiplied by a corresponding weight factor. Taking into account the magnitude of the output variables, the precedence of the position variables

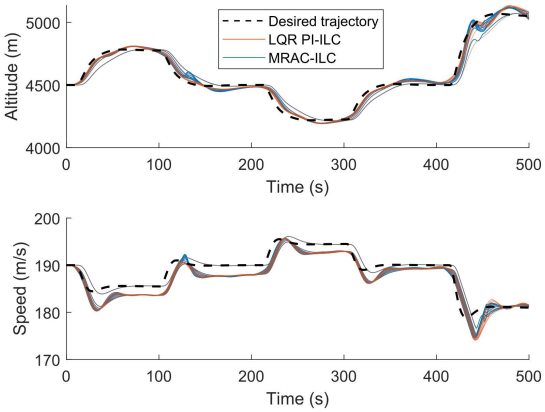


Figure 6: Experiment 2: Time evolution of the speed and altitude of the plant from iteration 1 to 9, before the plant model switch, using the ILC in combination with the MRAC augmentation of a baseline LQR PI controller and the LQR PI controller without MRAC augmentation.

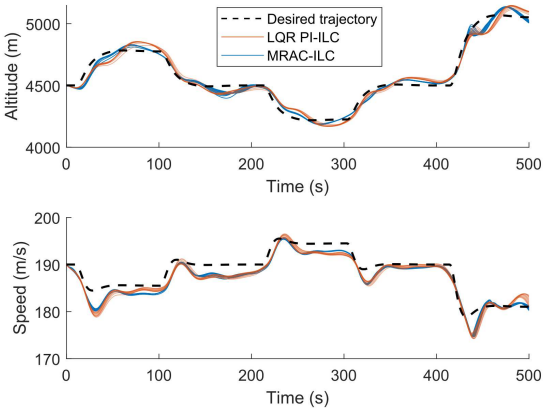


Figure 7: Experiment 2: Time evolution of the speed and altitude of the plant from iteration 10 on, after the plant model switch, using the ILC in combination with the MRAC augmentation of a baseline LQR PI controller and the LQR PI controller without MRAC augmentation.

over the speed, and the observed system behavior, the chosen weight factors are 0.48 for the speed, 0.002 for the horizontal position, and 0.01 for the altitude. Using the MRAC-ILC method, the initial output tracking error caused by the external disturbances is reduced in a few iterations of the ILC. The same occurs if the ILC is used in combination with the baseline LQR PI controller. This is due to the fact that during the first nine iterations there is a concordance between the reference and plant models, which in both cases is that of an A320 aircraft. However, after iteration 10, in which the plant model switches to that of a B767 aircraft, and there is a mismatch between reference model and plant model, using the MRAC-ILC method, a small increase in the output tracking error is observed after the plant model switch. On the contrary, using the LQR PI-ILC combination, a significantly larger output tracking error is observed after the plant model switch. It is interesting to point out that, in both cases, the ILC remains effective after the plant model switch, and the learning process continues until its convergence to the lower bound for the achievable weighted state error. The only difference is that the MRAC-ILC method is faster than the LQR PI-ILC combination, which requires more iterations to converge.

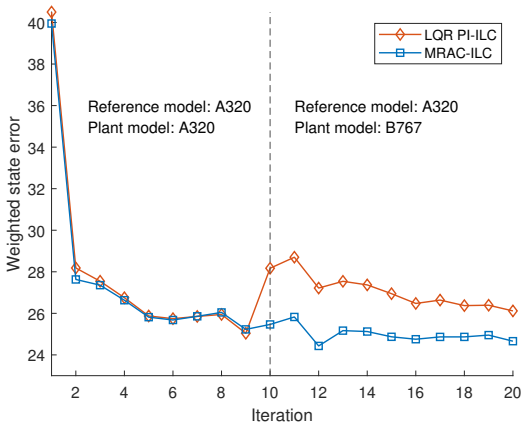


Figure 8: Experiment 2: Evolution of the weighted state error over iterations, using the ILC in combination with the MRAC augmentation of a baseline LQR PI controller and the LQR PI baseline controller without MRAC augmentation. During the first nine iterations, there is a concordance between reference and plant models, which in both cases is that of an A320. At iteration 10, the plant model switches to that of a B767.

*3) Experiment 3: MRAC-ILC with transfer learning among multiple aircraft with mismatch from the first iteration:* In this experiment, the whole MRAC-ILC method in Figure 1 is tested again when several different aircraft perform each iteration of the tracking task. As in Experiment 2, the reference model in the MRAC is that of an A320 aircraft with a baseline LQR PI controller, and the plant model is assumed to be affected by external disturbances, namely horizontal wind and measurement errors. The experiment is conducted in a demanding scenario where the successive iterations involve aircraft of different type and different initial mass are within a wide range. The goal of the experiment is to prove the effectiveness of the method in such an extreme case, so it can be assumed that it will also perform well in scenarios where the aircraft are not so different. Specifically, at each iteration starting from the first iteration, the plant model randomly changes to that of an A320, a B767, or an E195 with a random weight within their performance limits. Table I shows the sequence of aircraft and their weights performing each iteration. The desired trajectory and the command vector in the first iteration are the same as in Experiment 2.

The ultimate goal of this experiment is to prove that the deviations from the desired output trajectory experienced by the plant due to external disturbances can be amended by the ILC over iterations, learning from the deviations observed in previous executions of the tracking task, even if they are

performed from the very beginning by a random sequence of three different aircraft having random weights within their performance limits.

| Iteration | Aircraft | Mass (t) |
|---|---|---|
| 1 | B767 | 173.29 |
| 2 | B767 | 109.39 |
| 3 | A320 | 55.66 |
| 4 | B767 | 135.64 |
| 5 | E195 | 48.94 |
| 6 | E195 | 51.69 |
| 7 | A320 | 69.14 |
| 8 | A320 | 54.70 |
| 9 | B767 | 147.97 |
| 10 | A320 | 43.60 |
| 11 | B767 | 130.47 |
| 12 | A320 | 55.79 |
| 13 | B767 | 118.17 |
| 14 | E195 | 43.88 |
| 15 | B767 | 134.38 |
| 16 | B767 | 142.70 |
| 17 | B767 | 162.24 |
| 18 | B767 | 118.82 |
| 19 | E195 | 48.87 |
| 20 | E195 | 40.72 |

TABLE I. Experiment 3: Random sequence of aircraft and the corresponding random weights used at each iteration in the MRAC-ILC method.

Figure 9 shows the evolution of the path $x_e - h_e$ of the plant along all 20 iterations using the ILC in combination with the MRAC augmentation of a baseline LQR PI controller and the LQR PI controller without MRAC augmentation. Since the plant model switches at each iteration, starting from the first one, the path flown by the aircraft experiences variations. It can be observed that these variations are smaller, and the actual path of the plant remains closer to the desired path when the MRAC augmentation is active. In addition, since there is not a series of initial iterations with concordance between reference and plant models, as in Experiment 2, before switching the plant model, the path followed by the aircraft at the first iterations is more precise with the MRAC than without it. After the first iteration, the path followed by the aircraft gets closer to the desired path at each iteration with both control strategies. However, this progressive approach towards the desired path is faster with the MRAC-ILC scheme than with the LQR PI-ILC scheme.

Figure 10 shows the time evolution of the altitude and the speed of the plant along all 20 iterations using the ILC in combination with the MRAC augmentation of a baseline LQR PI controller and the LQR PI controller without MRAC augmentation. As in the previous experiments, greater importance is given in the ILC algorithm to precision in position than precision in speed. Therefore, the precision in tracking the desired speed is sacrificed in favor of the precision in tracking the horizontal position and the altitude. As a consequence, the speed is driven below the desired values despite being quite accurate in the first iteration, so the altitude can get closer to the desired values at each iteration. As in the previous figure, although there is variability in the flown trajectories due to the random change in the plant model at each iteration, the actual altitude is closer to the desired

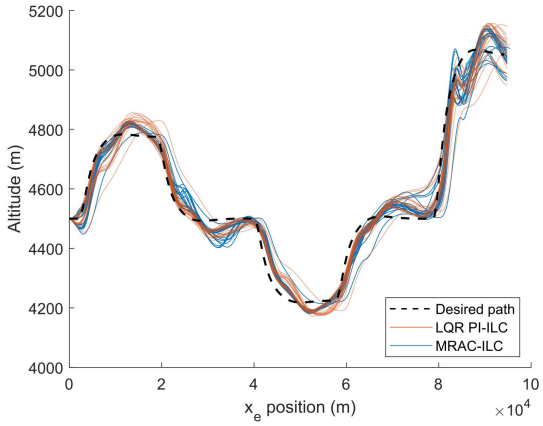


Figure 9: Experiment 3: Evolution of the path $x_e - h_e$ of the plant, the model of which randomly switches at each iteration, using the ILC in combination with the MRAC augmentation of a baseline LQR PI controller and the LQR PI controller without MRAC augmentation.

one for the most part of the trajectory when using the MRAC augmentation of a baseline LQR PI controller than without MRAC augmentation, whereas the actual speed is similar in both cases, although it experiences more variability with the LQR PI-ILC scheme.

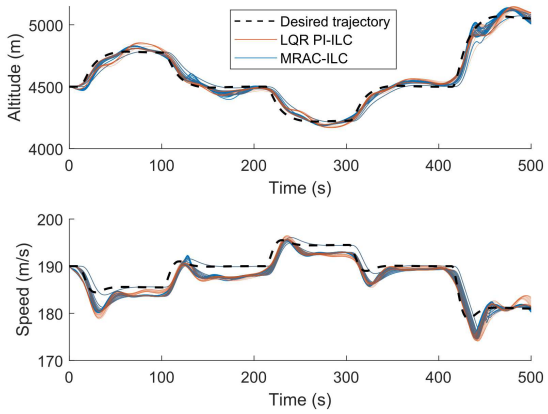


Figure 10: Experiment 3: Time evolution of the speed and altitude of the plant, the model of which randomly switches at each iteration, using the ILC in combination with the MRAC augmentation of a baseline LQR PI controller and the LQR PI controller without MRAC augmentation.

Finally, Figure 11 shows the evolution of the weighted state error over iterations using the ILC in combination with the MRAC augmentation of the baseline LQR PI controller and the LQR PI baseline controller without MRAC augmentation. It can be observed that the initial weighted state error is lower when using the ILC with the MRAC augmentation of the baseline controller since there is no concordance between the reference model and the plant model. In addition, the reduction of this error is faster with the MRAC-ILC scheme than with the LQR PI-ILC. The weighted state error

experiences variations with both control strategies. However, these variations are more pronounced when using the LQR PI-ILC than with the MRAC-ILC, in particular when the B767 aircraft is randomly selected since the performance characteristics of this aircraft are substantially different from those of both the A320 and the E195 aircraft.

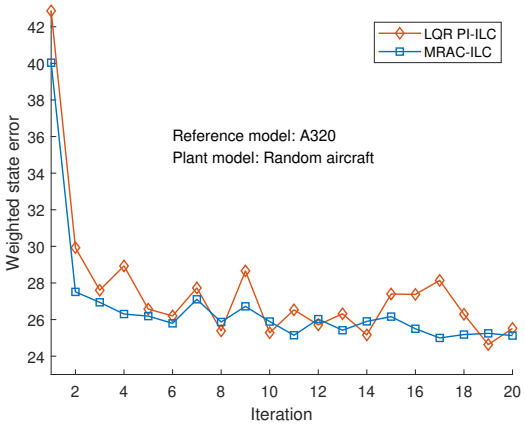


Figure 11: Experiment 3: Evolution of the weighted state error over iterations, using the ILC in combination with the MRAC augmentation of a baseline LQR PI controller and the LQR PI baseline controller without MRAC augmentation. The plant model randomly switches at each iteration.

*a) Statistical analysis of the performance of the MRAC-ILC.:* To statistically characterize the tracking performance of the ILC used in combination with the MRAC augmentation of the baseline LQR PI controller, the experiment described above is repeated 30 times and the average and the standard deviation of the weighted state error are computed. The results are compared with those obtained using the ILC in combination with the LQR PI baseline controller without MRAC augmentation.

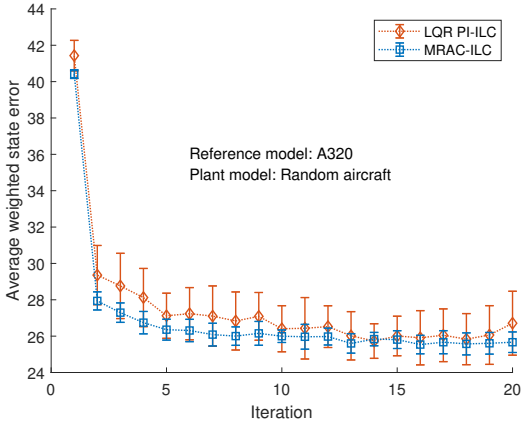


Figure 12: Experiment 3: Evolution of the average weighted state error and its standard deviation across 30 sets of iterations, using the LQR PI baseline controller and the MRAC adaptive controller. The plant randomly switches at each iteration.

Figure 12 shows the evolution of the average weighted state error and its standard deviation calculated across the 30 sets of 20 iterations with the ILC used in combination with the MRAC augmentation of the baseline LQR PI controller and the LQR PI controller without MRAC augmentation. Since there is not a series of initial iterations with concordance between reference and plant models before switching the plant model, the LQR PI-ILC is slower than the MRAC-ILC, reaching the convergence level several iterations after the MRAC-ILC, on average. The variations with respect to the average error are noticeably higher with the LQR PI-ILC approach. On the contrary, the MRAC-ILC scheme shows much smaller standard deviations consistently along all iterations.

These results demonstrate that the proposed MRAC-ILC scheme successfully reduces the external deviations affecting the flights by learning from previous executions of the same trajectory. Each iteration can be performed by different aircraft, with different performance parameters and weights, and the knowledge acquired can still be transferred to the following aircraft with small variations in the tracking error. As a consequence, the predictability of trajectory tracking is improved, making the proposed architecture suitable for real operation, where, in general, different aircraft perform a planned trajectory in the presence of disturbances.

## VI. Conclusion

The preliminary results of the experiments demonstrate the capability of the proposed MRAC-ILC method to improve the precision in tracking aircraft trjaectories consisting of a series of steps of different magnitude for both the speed and altitude, by learning from previous iterations. The MRAC forces the dynamically different aircraft to behave close to a similar reference model. This way, the ILC perceives them as a repetition-invariant dynamic system, enabling the learned trajectory knowledge to be transferred among different aircraft at each iteration, compensating for the recurrent disturbances affecting the flight. Higher precision in tracking the reference trajectory is achieved when using the MRAC augmentation of an LQR PI baseline controller as compared to the performance of the baseline controller without MRAC augmentation. Additionally, the former results in smoother variations in the output error, enhancing the predictability of the flown trajectory.

These encouraging results suggest that the MRAC-ILC could be successfully employed in tracking aircraft trajectories in realistic operational procedures, such as continuous climb and descent operations. Exploring this possibility is subject of current research.

The proposed method addresses one limitation of the ILC, which requires the system to be repetition-invariant, allowing different aircraft with different system dynamics to execute each consecutive flight. However, it does not solve the other limitation of the ILC, which also requires the trajectory to follow to be repetition-invariant. This aspect will be addressed in future research.

## REFERENCES


[1] A. Buelta, A. Olivares, and E. Staffetti, "Iterative learning control for precise aircraft trajectory tracking in continuous climb and descent operations," *IEEE Transactions on Intelligent Transportation Systems*, vol. 23, no. 8, pp. 10 481–10 491, 2022.

[2] A. Tayebi, "Model reference adaptive iterative learning control for linear systems," *International Journal of Adaptive Control and Signal Processing*, vol. 20, no. 9, pp. 475–489, 2006.

[3] S. Jingzhuo and W. Huang, "Model reference adaptive iterative learning speed control for ultrasonic motor," *IEEE Access*, vol. 8, pp. 181815–181824, 2020.

[4] B. Yuksek and G. Inalhan, "Reinforcement learning based closed-loop reference model adaptive flight control system design," *International Journal of Adaptive Control and Signal Processing*, vol. 35, no. 3, pp. 420–440, 2021.

[5] B. Altın and K. Barton, "Robust iterative learning for high precision motion control through $\mathcal{L}_1$ adaptive feedback," *Mechatronics*, vol. 24, no. 6, pp. 549–561, 2014.

[6] K. Pereida, R. R. P. R. Duivenvoorden, and A. P. Schoellig, "High-precision trajectory tracking in changing environments through $\mathcal{L}_1$ adaptive feedback and iterative learning," in *in Proceedings of the IEEE International Conference on Robotics and Automation*, Marina Bay Sands, Singapore, May 2017.

[7] K. Pereida, D. Kooijman, R. R. P. R. Duivenvoorden, and A. P. Schoellig, "Transfer learning for high-precision trajectory tracking through $\mathcal{L}_1$ adaptive feedback and iterative learning," *International Journal of Adaptive Control and Signal Processing*, vol. 33, no. 2, pp. 388–409, 2019.

[8] A. Buelta, A. Olivares, E. Staffetti, W. Aftab, and L. Mihaylova, "A Gaussian process iterative learning control for aircraft trajectory tracking," *IEEE Transactions on Aerospace and Electronic Systems*, vol. 57, no. 6, pp. 3962–3973, 2021.

[9] A. P. Schoellig, F. L. Mueller, and R. D'Andrea, "Optimization-based iterative learning for precise quadrocopter trajectory tracking," *Autonomous Robots*, vol. 33, no. 1-2, pp. 103–127, 2012.

[10] R. Tousain, E. van der Meche, and O. Bosgra, "Design strategy for iterative learning control based on optimal control," in *Proceedings of the 40th IEEE Conference on Decision and Control (Cat. No. 01CH37228)*, Orlando, FL, USA, December 2001.

[11] B. Bamieh, J. B. Pearson, B. A. Francis, and A. Tannenbaum, "A lifting technique for linear periodic systems with applications to sampled-data control," *Systems & Control Letters*, vol. 17, no. 2, pp. 79–88, 1991.

[12] E. Lavretsky and K. Wise, *Robust and Adaptive Control With Aerospace Applications*. Springer, 2013.

[13] D. G. Hull, *Fundamentals of Airplane Flight Mechanics*. Springer-Verlag, 2007.

[14] V. Mouillet, "User manual for the Base of Aircraft Data (BADA) Revision 3.14," EUROCONTROL Experimental Centre, Brétigny, France, Tech. Rep., 2017.